

The scanning light ion microprobe in Uppsala – Status in 2022

Gyula Nagy^{a,*}, Harry J. Whitlow^b, Daniel Primetzhofer^{a,b}

^a Department of Physics and Astronomy, Uppsala University, Box 516, S-751 20 Uppsala, Sweden

^b Tandem Laboratory, Uppsala University, Box 529, S-751 21 Uppsala, Sweden

ARTICLE INFO

Keywords:

Scanning nuclear microprobe
Micro-PIXE
Particle identification

ABSTRACT

The Scanning Light Ion Microprobe in Uppsala (SLIM-UP) was originally installed during 1989/90. Since then, the microprobe has undergone several minor and major modifications. The present configuration is a re-build of the SLIM-UP, that is now connected to the 5 MV tandem Pelletron® accelerator of the Tandem Laboratory, Uppsala University. We give an overview of the present status of the Uppsala microprobe facility, including a detailed description of the components and a recent resolution test. In addition, we present the most recent technical developments whereby, the system is able to quickly image large area samples, to reliably identify individual microparticles, and to analyse them separately. Optimal parameters for a certain system can be found by simple test measurements on dummy samples. Our test scenario comprises of Fe particles embedded in a light matrix, representing human tissue. We found a good compromise between the required analysis time and particle detection efficiency.

1. Introduction

Scanning nuclear microprobes focus MeV energy ion beams, commonly provided by an electrostatic particle accelerator, down to the micrometer lateral scale. Microprobes have found a wide variety of applications starting from microanalysis [1] towards implantation and micro-modification of materials [2]. Although there is no up-to-date database, according to the latest available information found, there are more than 50 nuclear microprobe laboratories around the world [3]. Most of them are used, at least partially, for elemental micro-analysis, which is based on the detection of the interaction products (such as particles or photons) of different interactions between the primary ion beam and the sample. These analysis techniques involve, among others, Particle-Induced X-ray Emission analysis (PIXE), Elastic/Rutherford backscattering spectrometry (EBS/RBS), Nuclear Reaction Analysis (NRA) and Scanning Transmission Ion Microscopy (STIM).

In Uppsala, such a scanning nuclear microprobe has been in operation since 1989/1990 [4]. Although there are many different types of microprobes developed and successfully used (e.g. focusing with a superconducting solenoid [5], plasma lens [6], etc.), the Uppsala microprobe is a typical facility which uses the most common solutions for object-forming, probe-forming and scanning. Originally, it was installed in The Svedberg Laboratory (TSL), where it was attached to a HVEE EN tandem Van de Graaff accelerator [7]. After the decommissioning of TSL, the beamline was re-built at the Ångström Laboratory

in 2002. At this time the microprobe was installed on the second beamline of the tandem Pelletron® accelerator of the Tandem Laboratory, Uppsala University. Since then the end-station has been in use for ion-beam analysis purposes in an interdisciplinary/multidisciplinary manner, including fusion-related research (e.g. [8,9]), forensic science [10] and materials science [11]. An ongoing scientific project, for instance, combines ion beam analysis and materials chemistry to non-destructively study the depth-resolved distribution of post-synthetically introduced active sites in metal-organic framework (MOF) single crystals [12,13]. Since the need for spatially resolved ion beam analysis has attracted increasing interest from researchers, a major upgrade of the Uppsala microprobe has been started, including the design and installation of a new target chamber, an in-air beam extension, new detectors, etc. In this paper we report on the present configuration, prior to the planned major upgrade.

2. Description of the system

2.1. Hardware

The Uppsala scanning nuclear microprobe is now located at the Ångström Laboratory. It is connected to the 5 MV tandem Pelletron® accelerator (model 15SDH-2, delivered by National Electrostatic Corporation) of the Tandem Laboratory, Uppsala University. A detailed description about the whole Laboratory and its activities can be found in

* Corresponding author.

<https://doi.org/10.1016/j.nimb.2022.10.017>

Received 25 September 2022; Accepted 25 October 2022

Available online 10 November 2022

0168-583X/© 2022 The Authors. Published by Elsevier B.V. This is an open access article under the CC BY license (<http://creativecommons.org/licenses/by/4.0/>).

Ref. [14], in the followings we focus only on the nuclear microprobe facility.

The schematic drawing of the microprobe is shown in Fig. 1. The main components were delivered by Oxford Microbeams Ltd [15]. The object forming apertures and collimator apertures are the standard OM10 products. The object to collimator distance is 6.65 m, resulting in a 7.56 m length of the full system. The OM50 magnetic quadrupole focusing lenses are arranged in the standard Oxford-triplet C-D-C configuration. The theoretical demagnification factor of this layout is approximately 80×20 (horizontal \times vertical). The beam is raster-scanned over the sample by OM25 ferrite cored pre-lens deflector coils, which are driven by the OM40e 2-channel scan amplifier. Event mode data collection is performed by an MPA-3 data acquisition system (Fast ComTec GmbH), which can handle 8 individual ADC channels simultaneously. The analogue voltage signal that controls the scan amplifier is generated by a NI PCIe (model 6323) DAQ card. The generated voltage signal is then split and is driven i) into the OM40e scan amplifier unit and ii) into two independent ADCs (one for the X and one for the Y scan signal), operating in sampling voltage analysis (SVA) mode in order to record the scan coordinates for mapping using the MPA-3 data acquisition system. Maps of the chemical composition are built up by collecting detector counts in selected regions of interests in coincidence with the actual scan signal levels.

The largest area that can be mapped by a beam scan depends on the magnetic rigidity of the ion beam to be used. For the usual beam of 2 MeV protons it is around $2 \text{ mm} \times 2 \text{ mm}$. Anything above this can be mapped by a mosaic combination of stage scanning and beam scanning, i.e. tiling the sample into sub-regions, mapping them separately and then stitching the maps together. The stage has three motorised translational axes, with a total of $25 \text{ mm} \times 50 \text{ mm} \times 25 \text{ mm}$ (horizontal \times vertical \times longitudinal) range. The stage can be programmed to scan a batch of samples or a single but tiled sample automatically.

Beam current measurements can be performed in several ways. The entire target chamber can be used as a Faraday-cup since the chamber is electrically isolated from the beamline and chamber support. The current can also be measured from the sample holder, where a suppression voltage might be applied to reduce the measurement uncertainty caused by the generated secondary electrons. In the case of thin samples, a Faraday-cup placed in transmission geometry can be employed. The collected current is then integrated by a charge digitizer, and counted by the MPA-3 data acquisition system through a separate ADC channel.

The target chamber, illustrated in Fig. 2, is home-made, based on the Oxford Microbeams design. It has an octagonal shape design with 7 free ports (one is occupied by the beam tube) for detectors, optical microscope, feedthroughs, etc. Several ion-beam analytical techniques are implemented and are operated routinely. RBS/EBS and particle-NRA are carried out using an annular-type surface barrier detector (thickness: $1500 \mu\text{m}$, solid angle: 0.39 sr). A retractable Si(Li) detector (Princeton Gamma-Tech) with 30 mm^2 active area, placed at the 135° port is used for PIXE analysis. Easily replaceable filter foils of different thicknesses are used to prevent detector damage due to backscattered ions. For STIM and ERDA, we use PIN diodes (Hamamatsu) placed in a properly shielded case. The unit can be easily moved to the on-axis or off-axis configuration, or can be easily removed when not needed.

2.2. Software tools

For fitting the spectra of different ion beam analysis techniques, the most advanced software packages are available. For PIXE we use the GUPIX [16] and GeoPIXE [17] programs. The former can be used only for spectrum fitting, while the latter can build up element maps, too, based on the scan-controlling signals (i.e. beam position) collected in coincidence with the detector counts. For RBS/EBS, ERDA and NRA we use SIMNRA [18]. A home-developed software, PyList [19] is used to process the binary list mode files generated by the Fast MPA-3 system. PyList is also capable of filtering data based on different coincidence criteria, selecting 1D slices (e.g. energy range in a spectrum, line scan in a 2D map, etc.) or 2D regions (e.g. region in a 2D element map) and arbitrarily combining them. The processed data can be exported to several different file formats which might be then further processed with e.g. the above-mentioned data fitting software, but can also be visualized in publication quality based on the pyplot plotting library.

2.3. Resolution test

A test of the resolution, after proper alignment of the focusing quadrupole lenses, was carried out using a 2 MeV H^+ beam. A 1000 mesh TEM grid (Ted Pella, Inc.) was used as a standard. The resolution test was performed in two modes: high current mode (beam intensity of several hundred pA), suitable for PIXE, RBS and off-axis STIM analysis; and low current mode (beam intensity of $\approx 1\text{--}2000$ ions/s), suitable for on-axis STIM analysis. The beam current was reduced by more stringent spatial filtering by reducing the objective and collimator apertures which had the effect of reducing the size of the beam spot. The focused beam was line-scanned over the grid bar, and the signal originating from the grid material ($\text{Cu K}\alpha$ X-ray lines) or the transmitted direct beam was detected as a function of the beam position. The procedure was repeated for both scanning axes. Assuming a Gaussian-shaped beam profile, the beam resolution, which is defined by the full width at half maximum (FWHM), was obtained by fitting an error-function (ERF) to the curves. The measurements are illustrated in Fig. 3. The results show that the beam spot size (FWHM) in high-current mode is $3.3 \mu\text{m} \times 2.0 \mu\text{m}$, while in low current mode it is $1.5 \mu\text{m} \times 1.0 \mu\text{m}$.

Although the beam spot size is not outstanding among microprobes using a similar focusing system, we note that this is a routinely available spot size without any complex and time-consuming preparation or maintenance (except for the lens alignment) made prior to the tests.

2.4. Recent developments - Fast automatic mapping of microparticles in large samples

Recent applications include locating a few small microparticles in large area samples, of the order of tens of mm^2 . Usually, the composition of these particles needs to be determined, but the matrix is less important. Examples comprise e.g. Ti microparticles in human tissue samples [20] originating from bone implants, micro-crystals randomly grown on large substrates, etc. If individual small microparticles are deeply buried, for example, in the tissue sections, they are not visible on optical microscope pictures, which confounds optical identification of the

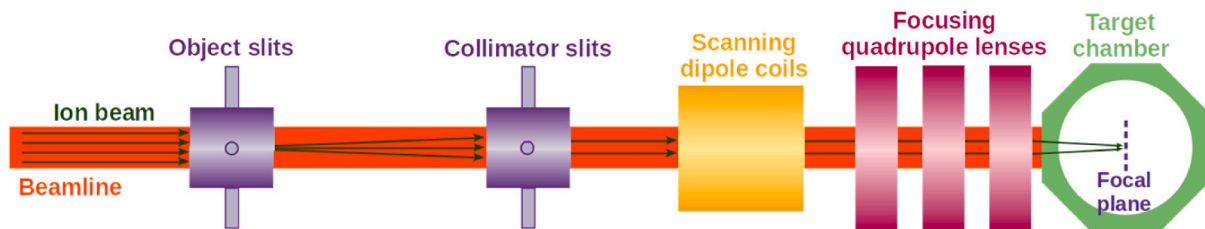


Fig. 1. Schematic drawing (not to scale) of the Uppsala scanning nuclear microprobe.

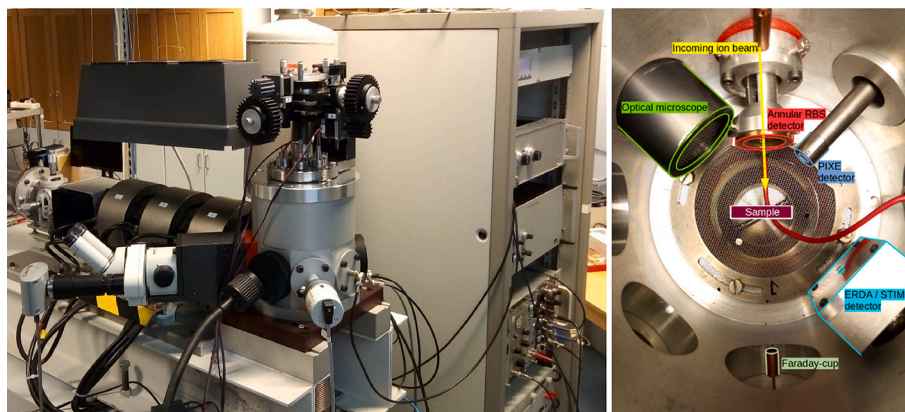


Fig. 2. Photo of the Uppsala scanning nuclear microprobe (left) and the inside of the target chamber (right).

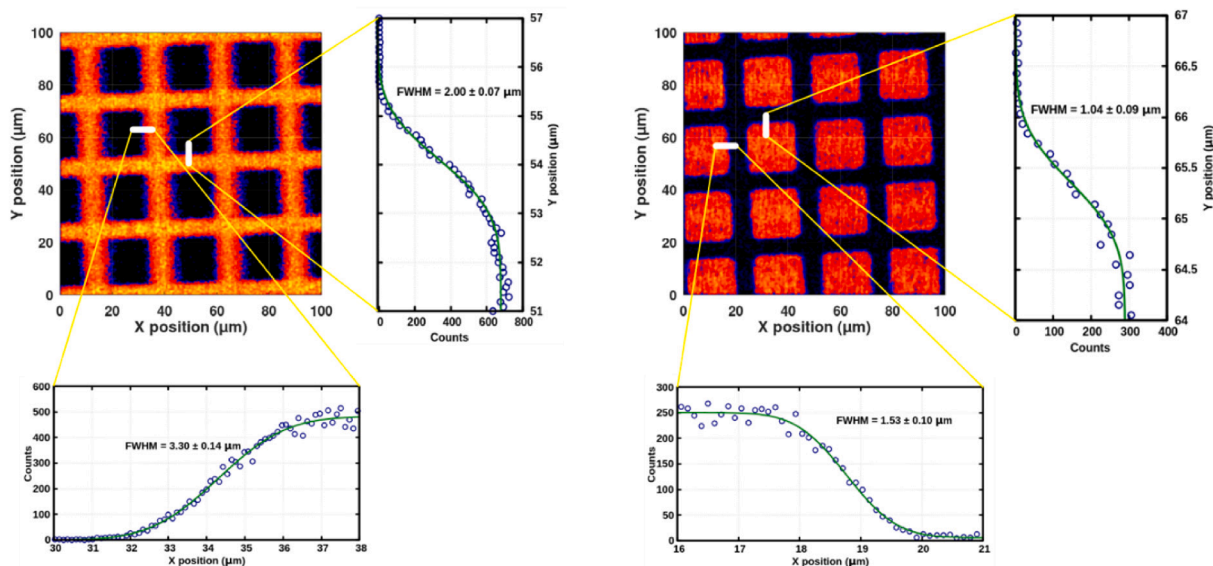


Fig. 3. Maps of the 1000 mesh Cu calibration grid and line scan profiles at the indicated regions. Scan size: $100 \times 100 \mu\text{m}^2$. Left: high-current mode (PIXE Cu map); Right: low-current mode (on-axis STIM E_0 map).

particles. Here we present our new, automated measurement system that makes the fast mapping of the microparticles in large samples feasible.

The sample manipulator can be programmed to scan a batch of samples. For a single sample, if it is larger than the maximum scan size for a given beam, the sample area is scanned using mosaic imaging with combined stage scanning and beam scanning. Microparticles are automatically identified during the measurements by processing any selected IBA map using a digital image processing technique. After a pre-defined ion fluence is delivered on the sample, a Hough-transform is performed on the selected IBA map in order to locate circular-like objects within a given size-range, and a new measurement starts around this region with the desired statistics. An optional filtering might be applied to increase sensitivity. The optimal value of the delivered fluence for this procedure can be determined in a test measurement as described in the following, making real measurements more time-effective. The test measurement was carried out using a 2 MeV H^+ beam, as it represents a typical choice for PIXE measurements when medium-heavy elements are present in a light matrix.

To test the procedure, micro-sized Fe particles (size ranging from $\approx 1 \mu\text{m}$ to tens of μm) were mixed with cyanoacrylate adhesive and applied on a Si substrate. This procedure resulted in a model sample of microparticles randomly distributed in a light matrix, similar to the atomic

composition of human tissue, still well visible under a conventional light microscope. Then, Fe PIXE maps were acquired from a randomly chosen region of $1 \text{ mm} \times 1 \text{ mm}$ area, using different ion fluences, and the particle detection algorithm was applied on each. Pile-up of X-rays from the substrate was mitigated by a filter in front of the Si-Li detector which strongly attenuates the low energy 1.74–1.84 keV characteristic X-rays from Si compared to the higher energy 6.40–7.06 keV characteristic X-rays from Fe. The Fe PIXE maps with the identified microparticles, together with an optical microscope image of a selected region, are illustrated in Fig. 4. The results show that after an ion fluence as low as $200 \text{ nC}/\text{mm}^2$, microparticles with size as small as $1.5 \mu\text{m}$ in diameter could be located. This small particle size is equivalent to a sensitivity of approximately 0.1 ppm. This ion fluence represents a good compromise between measurement time and detection efficiency, since delivering this fluence with a conventional microbeam current of a few hundred picoamperes takes only a few minutes per square millimeter.

3. Conclusions

We reported the present status of the Uppsala scanning nuclear microprobe facility, located at the Tandem Laboratory of Uppsala University. The available beam resolution is a few-micrometers in the high-current mode, and it is slightly above one micrometer in the low current

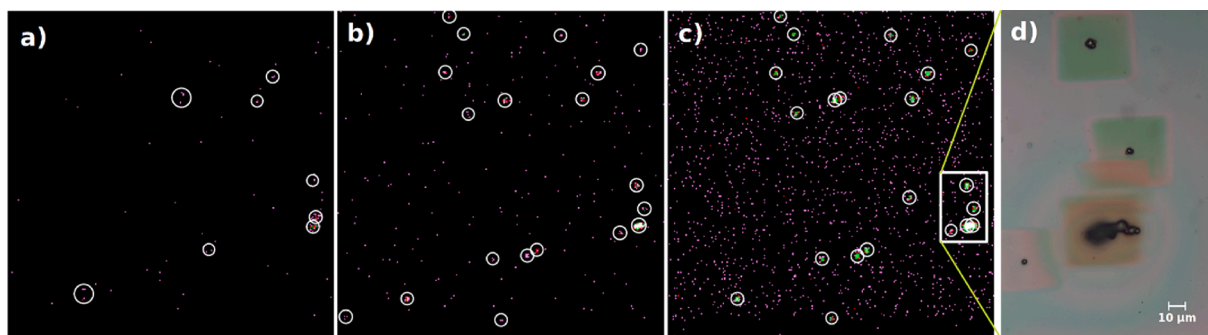


Fig. 4. Fe PIXE maps after a) 50 nC/mm²; b) 200 nC/mm² and c) 2000 nC/mm² delivered ion fluence. d) Optical microscope picture of the marked region of interest. The discolored squares are changes in the cyanoacrylate adhesive induced by the proton beam.

mode. Standard ion-beam analytical techniques, such as PIXE, RBS, STIM, ERDA and particle-NRA are implemented and are used in a daily operation. With the help of the most recent developments, large area samples and/or a batch of samples can be mapped in a fully automated manner, permitting effectively scanning areas of several cm² over duration of days without the need of operator interception. Micro-particles can be identified based on digital image processing techniques performed on any selected IBA maps. The method ensures a time-efficient way for localizing and analysing micro-particles in large samples. Test measurements on dummy samples showed that metal micro-particles embedded in a light matrix with concentration below the ppm level can be identified using micro-PIXE.

Declaration of Competing Interest

The authors declare that they have no known competing financial interests or personal relationships that could have appeared to influence the work reported in this paper.

Acknowledgements

Support of accelerator operation by the Swedish Research Council VR is acknowledged (VR-RFI contract #2019-00191).

References

- [1] C. Jeynes, Total IBA - Where are we? *Nucl. Instr. Meth. Phys. Res. B* 271 (2012) 107–118, <https://doi.org/10.1016/j.nimb.2011.09.020>.
- [2] J.A. van Kan, A.A. Bettiol, K. Ansari, E.J. Teo, T.C. Sum, F. Watt, Proton beam writing: a progress review, *Int. J. Nanotechnol.* 1 (4) (2004) 464, <https://doi.org/10.1504/IJNT.2004.005980>.
- [3] M.B.H. Breese, The nuclear microprobe, *Nucl. Phys. News* 19 (2009) 33–37, <https://doi.org/10.1080/10506890902958943>.
- [4] T. Sunde, J. Nyström, U. Lindh, The new scanning nuclear microprobe in Uppsala, *Nucl. Instr. Meth. Phys. Res. B* 54 (1991) 80–83, [https://doi.org/10.1016/0168-583X\(91\)95495-Y](https://doi.org/10.1016/0168-583X(91)95495-Y).
- [5] C.J. Maggiore, The Los Alamos nuclear microprobe with a superconducting solenoid final lens, *Nucl. Instr. Meth. Phys. Res. B* 191 (1981) 199–203, [https://doi.org/10.1016/0029-554X\(81\)91005-3](https://doi.org/10.1016/0029-554X(81)91005-3).
- [6] H.W. Lefevre, R.C. Connolly, G. Sieger, J.C. Overley, Scanning MeV-ion microprobe for light and heavy ions, *Nucl. Instr. Meth. Phys. Res. B* 218 (1–3) (1983) 39–42, [https://doi.org/10.1016/0167-5087\(83\)90951-1](https://doi.org/10.1016/0167-5087(83)90951-1).
- [7] S. Holm, A. Johansson, S. Kullander, D. Reistad, New accelerators in Uppsala, *Phys. Scr.* 34 (6A) (1986) 513–532, <https://doi.org/10.1088/0031-8949/34/6A/007>.
- [8] P. Petersson, H. Bergsäker, G. Possnert, J.P. Coad, S. Koivuranta, J. Likonen, Ion beam micro analysis of deposits at tokamak divertor surfaces, *Nucl. Instr. Meth. Phys. Res. B* 268 (11–12) (2010) 1838–1841, <https://doi.org/10.1016/j.nimb.2010.02.025>.
- [9] P. Petersson, G. Possnert, M. Rubel, T. Dittmar, B. Pégourié, E. Tsitrone, E. Wessel, An overview of nuclear micro-beam analysis of surface and bulk fuel retention in carbon-fibre composites from Tore Supra, *J. Nucl. Mater.* 415 (1) (2011) S761–S764, <https://doi.org/10.1016/j.jnucmat.2010.10.044>.
- [10] V. Mathayan, M. Sortica, D. Primetzhofner, Determining the chronological sequence of inks deposited with different writing and printing tools using ion beam analysis, *J. Forensic Sci.* 66 (2021) 1401–1409, <https://doi.org/10.1111/1556-4029.14705>.
- [11] H.J. Whitlow, G. Nagy, Micro-Particle Induced X-Ray Emission (PIXE) study of lead-free and lead-based solders and interactions with copper wires, *Phys. Status Solidi A*, revised manuscript.
- [12] V. Paneta, et al., Characterization of compositional modifications in metal-organic frameworks using carbon and alpha particle microbeams, *Nucl. Instr. Meth. Phys. Res. B* 404 (2017) 198–201, <https://doi.org/10.1016/j.nimb.2017.01.058>.
- [13] B.D. McCarthy, T. Liseev, M.A. Sortica, V. Paneta, W. Gschwind, G. Nagy, S. Ott, D. Primetzhofner, Elemental depth profiling of intact metal–organic framework single crystals by scanning nuclear microprobe, *J. Am. Chem. Soc.* 143 (44) (2021) 18626–18634, <https://doi.org/10.1021/jacs.1c08550>.
- [14] P. Ström, D. Primetzhofner, Ion beam tools for nondestructive in-situ and in-operando composition analysis and modification of materials at the Tandem Laboratory in Uppsala, *J. Instrum.* 17 (2022) P04011, <https://doi.org/10.1088/1748-0221/17/04/P04011>.
- [15] <http://www.microbeams.co.uk/>.
- [16] J.L. Campbell, D.J.T. Cureatz, E.L. Flannigan, C.M. Heirwegh, J.A. Maxwell, J. L. Russell, S.M. Taylor, The Guelph PIXE software package V, *Nucl. Instr. Meth. Phys. Res. B* 499 (2021) 77–88, <https://doi.org/10.1016/j.nimb.2021.05.004>.
- [17] C.G. Ryan, J.S. Laird, L.A. Fisher, R. Kirkham, G.F. Moorhead, Improved Dynamic Analysis method for quantitative PIXE and SXRF element imaging of complex materials, *Nucl. Instr. Meth. Phys. Res. B* 363 (2015) 42–47, <https://doi.org/10.1016/j.nimb.2015.08.021>.
- [18] M. Mayer, Improved physics in SIMNRA 7, *Nucl. Instr. Meth. Phys. Res. B* 332 (2014) 176–180, <https://doi.org/10.1016/j.nimb.2014.02.056>.
- [19] P. Ström, Material characterization for magnetically confined fusion: Surface analysis and method development, Doctoral Thesis, KTH Royal Institute of Technology, 2019, page 64. <http://www.divaportal.org/smash/get/diva2:1277095/FULLTEXT04.pdf>.
- [20] H.J. Whitlow, N. Henderson, R. Greco, N. Deoli, K.M. Smith, K. Morgan, F. Villinger, PIXE studies of normal and SIV-infected rhesus macaque tissues: investigations of particulate matter. Proc. 25th International Conference on Ion Beam Analysis & 17th International Conference on Particle Induced X-ray Emission & International Conference on Secondary Ion Mass Spectrometry, *J. Phys. Conf. Series*, 2022 (In press).

Further reading